arXiv:1209.3667v1 [cond-mat.stat-mech] 17 Sep 2012

Efficiencies of a molecular motor: A generic hybrid model applied to the F_1–ATPase

Eva Zimmermann and Udo Seifert

II. Institut für Theoretische Physik, Universität Stuttgart, 70550 Stuttgart, Germany

Abstract. In a single molecule assay, the motion of a molecular motor is often inferred from measuring the stochastic trajectory of a large probe particle attached to it. We discuss a simple model for this generic set-up taking into account explicitly the elastic coupling between probe and motor. The combined dynamics consists of discrete steps of the motor and continuous Brownian motion of the probe. Motivated by recent experiments on the F_1–ATPase, we investigate three types of efficiencies both in simulations and a Gaussian approximation. Overall, we obtain good quantitative agreement with the experimental data. In particular, we clarify the conditions under which one of these efficiencies becomes larger than one.

PACS numbers: 87.16.Nn, 05.40.Jc, 05.70.-a

1. Introduction

Molecular motors are protein complexes of the size of nanometers that convert chemical energy into mechanical motion [1, 2]. Operating in an aqueous solution they exhibit stochastic dynamics and energetics due to the influence of thermal fluctuations. Unbalanced concentrations of the molecules providing chemical energy as input cause the motor proteins to operate under nonequilibrium conditions which induces a rectified motion with non–zero average velocity. Consequently, molecular motors are often modelled using Langevin, Fokker–Planck or master equations. The so called ratchet models combine continuous diffusive spatial motion with stochastic switching between different potentials corresponding to different chemical states [3, 4]. Alternatively, transitions among a discrete state space governed by master equations provide another possibility to model molecular motors [5, 6, 7, 8, 9].

A quantity of general interest is the efficiency of such stochastic machines [10, 11, 12, 13, 14]. For motor proteins, different kinds of efficiencies can be defined depending on whether one focuses on the work against an external force, i.e., thermodynamic efficiency or whether work against viscous friction is also taken into account like in the Stokes or generalized efficiency [15, 16, 17, 18, 19, 20].

Experimentally, the properties of motor proteins can be investigated in single molecule experiments by attaching probe particles of the size of micrometers to the motor protein and by observing the trajectories of the probes. Additionally, such probes

allow to exert forces on these motor proteins [21, 22, 23, 24]. Literally speaking, in these assays one cannot observe the motion of the motor directly but rather has to infer its properties from analyzing the trajectory of the probe particle. Generically, some elastic linker couples these two elements. Inferring properties of the motor protein requires to consider the interaction effects that depend on the linkage between motor protein and probe [25, 26, 27, 28, 29, 30, 31, 32].

In the present paper, we discuss a minimal hybrid model for such a motor protein assay that includes this elastic link explicitly. The motor protein and the probe will be modelled as two degrees of freedom moving along a spatial coordinate. In particular, we investigate different kinds of efficiencies used previously to describe the energetics of molecular motors and compare our results quantitatively to recent experiments of the rotary motor protein F_1–ATPase [33, 34, 35, 36]. Previous theoretical modelling of F_1–ATPase using a discrete state model as well as a ratchet model assuming the probe to stick directly at the motor has especially focussed on the dependence of the rotational behaviour on friction, external forces, nucleotide concentrations and temperature as well as on chemical and thermodynamic efficiency and the fluctuation theorem [37, 38]. Detailed modelling of the rotary mechanism and the involved subunits can be found in [39, 40].

This particularly well studied molecular motor consists of three α and three β subunits arranged around a central γ shaft [41]. Binding and hydrolysis of an ATP molecule at a β subunit drives a rotation of the γ shaft of 120° [21] which has been observed to consist of two substeps of 90° and 30° [42]. An external torque exerted on the γ shaft (as experimentally done in [23] or by the F_o part within the cell) induces ATP synthesis. Coupled to the membrane embedded F_o part, F_1–ATPase provides ATP for further hydrolysis reactions therefore being an important part in the energy transfer of cells. Experimental observations of the F_1–ATPase in the hydrolysis direction include the measurements of different kinds of efficiencies. The Stokes efficiency, a Stokes efficiency confined to single jumping events and the thermodynamic efficiency, especially at stall conditions, have been investigated [43, 44, 34]. These experiments led to values for the Stokes efficiency and the thermodynamic efficiency of almost 1 suggesting that the F_1–ATPase can use almost the complete chemical energy either to drive the probe through a viscous medium or to perform work against an external force. Recently, a measure of the efficiency that takes explicitely care of fluctuations was introduced [33]. The definition of efficiency used there also provided values close to 1 for the examined parameters. Our analysis will show that the latter efficiency can easily reach values larger than 1.

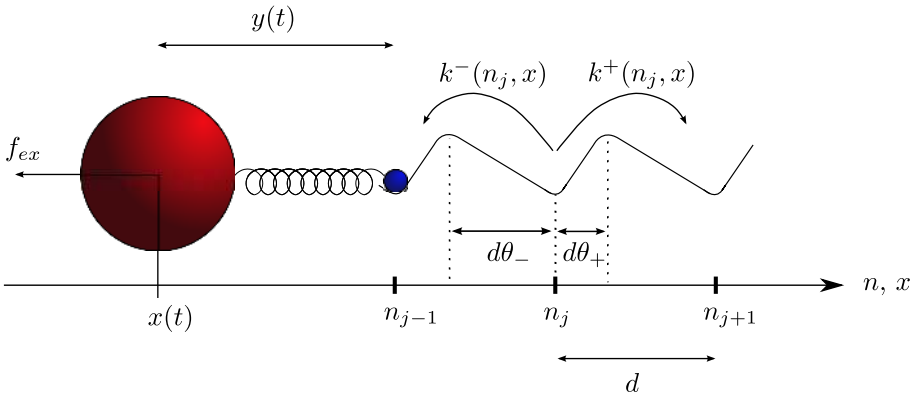

Figure 1. Schematic representation of the motor protein (blue) with attached probe (red). The instantaneous distance between motor protein and probe is denoted by $y(t)$. The probe moves along a continuous spatial coordinate $x(t)$ an is subject to an external force $f_{\rm ex}$. With transition rates $k^{\pm}(n_j, x)$ the motor protein jumps at times τ_j between discrete states n_j separated a distance d. The load sharing factors θ_+ and θ_- indicate the position of an underlying unresolved potential barrier relative to the potential minimum.

2. Hybrid–Model

2.1. Single molecule dynamics

The one–dimensional model we will use to describe a molecular motor with an attached probe particle consists of two degrees of freedom representing the motor protein at position $n(t)$ and the probe at position $x(t)$, respectively, see figure 1. For a rotary motor like the F_1–ATPase, the rotary motion is mapped to a linear one for simplicity. Both constituents are linked via a harmonic potential

$$V(n,x) = \frac{\kappa}{2}(n-x)^2 \tag{1}$$

with spring constant κ, where we have included a possible rest length of the linker into the definition of x.

The motion of the probe particle is described by an overdamped Langevin equation with friction coefficient γ and constant external force $f_{\rm ex}$,

$$\dot{x}(t) = (-\frac{\partial V}{\partial x} - f_{\rm ex})/\gamma + \zeta(t), \tag{2}$$

including the random force $\gamma\zeta(t)$ that the solvent exerts on the probe. The thermal fluctuations are assumed to be Gaussian white noise with zero mean and correlations $\langle\zeta(t_1)\zeta(t_2)\rangle = 2k_{\rm B}T\delta(t_1-t_2)/\gamma$ where $k_{\rm B}$ is Boltzmann's constant and T the temperature of the solvent.

The motor protein jumps at times τ_j from n_j to $n_j \pm d$ with transition rates $k^{\pm}(n_j, x)$, hydrolyzing (or synthesizing) one ATP molecule per jump which corresponds to tight mechanochemical coupling. In this minimal model, we take into account only one chemical state. The transition rates have to fulfill a local detailed balance condition

of the form

$$\frac{k^+(n,x)}{k^-(n+d,x)} = \exp[(\Delta\mu - V(n+d,x) + V(n,x))/k_{\rm B}T] \tag{3}$$

where we assume that the jumps of the motor protein take place instantaneously. The free energy change of the solvent

$$\Delta\mu \equiv \mu_{\rm ATP} - \mu_{\rm ADP} - \mu_{\rm P_i} \tag{4}$$

is associated with ATP turnover. Implementing mass action law kinetics and the concept of a barrier in the potential of mean force for the unresolved chemical steps, the individual rates become

$$\begin{aligned} k^+(n,x) &= k^{\rm eq} \exp[\Delta\mu_{\rm ATP}/k_{\rm B}T] \exp[\frac{1}{k_{\rm B}T} \int_n^{n+d\theta_+} -\frac{\partial V(n,x)}{\partial n}\,{\rm d}n] \\ &= k^{\rm eq} \exp[\Delta\mu_{\rm ATP}/k_{\rm B}T] \exp[(-\kappa d^2\theta_+^2/2 - \kappa(n-x)d\theta_+)/k_{\rm B}T] \end{aligned} \tag{5}$$

and

$$\begin{aligned} k^-(n,x) &= k^{\rm eq} \exp[(\Delta\mu_{\rm ADP} + \Delta\mu_{\rm P_i})/k_{\rm B}T] \exp[\frac{1}{k_{\rm B}T} \int_n^{n-d\theta_-} -\frac{\partial V(n,x)}{\partial n}\,{\rm d}n] \\ &= k^{\rm eq} \exp[(\Delta\mu_{\rm ADP} + \Delta\mu_{\rm P_i})/k_{\rm B}T] \exp[(-\kappa d^2\theta_-^2/2 + \kappa(n-x)d\theta_-)/k_{\rm B}T] \end{aligned} \tag{6}$$

with

$$\Delta\mu_i \equiv \mu_i - \mu_i^{\rm eq} = k_B T \ln(c_i/c_i^{\rm eq}) \tag{7}$$

and c_i the concentrations of the nucleotides (i = ATP, ADP, P_i). Here, the transition rate $k^{\rm eq}$ applies to equilibrium concentrations of nucleotides. The load sharing factors θ_+ and θ_-, with $\theta_+ + \theta_- = 1$, depend on the unresolved shape of the free-energy landscape of the motor protein [5, 45].

2.2. Fokker–Planck equation

The transition rates, as well as the force the motor protein exerts on the probe, depend on the distance

$$y(t) \equiv n(t) - x(t) \tag{8}$$

between motor and probe. The corresponding probability density $p(y,t)$ obeys the Fokker–Planck–type equation

$$\begin{aligned} \partial_t p(y,t) = {} & k^+(y-d)\,p(y-d,t) + k^-(y+d)\,p(y+d,t) - (k^+(y) + k^-(y))\,p(y,t) \\ & + \partial_y((\kappa y - f_{\rm ex})\,p(y,t) + k_{\rm B}T\partial_y\,p(y,t))/\gamma, \end{aligned} \tag{9}$$

which contains in the first line the contributions from the transitions of the motor protein and in the second line drift and diffusion of the probe particle.

For large t and constant nucleotide concentrations, the system reaches a stationary state with time independent $p^s(y)$ and constant mean velocity $\langle\dot{n}\rangle = \langle\dot{x}\rangle \equiv v$ with

$$\langle\dot{x}\rangle = (\kappa\langle y\rangle - f_{\rm ex})/\gamma \tag{10}$$

and

$$\langle \dot{n} \rangle = d\langle k^+(y) - k^-(y) \rangle \tag{11}$$

where $\langle ... \rangle$ denotes the average using the stationary distribution $p^s(y)$, which, however, cannot be determined analytically.

3. Efficiencies

3.1. First law: single trajectory

Following the concept of stochastic thermodynamics [46, 47] one can assign a first law on the level of a single trajectory. If the probe moves a small distance Δx, the first law becomes

$$\Delta q_{\rm P} = (-\frac{\partial V}{\partial x} - f_{\rm ex})\Delta x = (\kappa y - f_{\rm ex})\Delta x \tag{12}$$

where $\Delta q_{\rm P}$ is the heat dissipated by the probe, $f_{\rm ex}\Delta x$ is the work against the external force and $(\partial_x V)\Delta x$ the change of the internal energy of the spring due to the motion of only the probe. A jump of the motor protein gives rise to a first law in the form of [48]

$$\begin{aligned} 0 &= \Delta V + \Delta E_{\rm Sol} + \Delta q_{\rm M} \\ &= \Delta V - \Delta\mu + T\Delta S_{\rm Sol} + \Delta q_{\rm M} \end{aligned} \tag{13}$$

without a contribution of the internal energy of the motor as its internal energy does not change in the one–state model. The change of the internal energy of the spring is given by

$$\Delta V \equiv V(n \pm d, x) - V(n, x) \tag{14}$$

where the sign depends on the the direction of the jump. Due to ATP turnover, the internal energy of the solution changes by $\Delta E_{\rm Sol} = -\Delta\mu + T\Delta S_{\rm Sol}$, where $\Delta S_{\rm Sol}$ is the change of the entropy of the solution. The heat dissipated by the motor protein in this transition is denoted by $\Delta q_{\rm M}$.

3.2. First law: ensemble average

On average, the chemical energy gained from ATP consumption that involves changes of the entropy of the solvent will be dissipated as heat Q in the environment and/or is delivered as work against the external force. In the stationary state, the internal energy of the spring is constant on average. Taking the average rates of (12) and (13) and summing the two contributions, this first–law condition can be expressed as

$$\dot{\Delta\mu} = \dot{Q}_{\rm P} + \dot{Q}_{\rm M} + T\dot{S}_{\rm Sol} + f_{\rm ex}v \tag{15}$$

where the dot denotes a rate and

$$\dot{\Delta\mu} \equiv -\langle \dot{F}_{\rm Sol} \rangle = \Delta\mu v/d \tag{16}$$

is the rate of free energy consumption. The rate of dissipated heat $\dot{Q} = \dot{Q}_{\rm P} + \dot{Q}_{\rm M}$ has two contributions. First, the heat flow through the motor protein is given by

$$\dot{Q}_{\rm M} \equiv \langle \dot{q}_{\rm M} \rangle = \dot{\Delta}\mu - \dot{V}_n - T\dot{S}_{\rm Sol}, \tag{17}$$

representing the fact that while jumping, the motor protein uses free energy from the hydrolysis to load the spring which corresponds to a change of the internal energy of the spring $\dot{V}_n$ with

$$\dot{V}_n \equiv \int_{-\infty}^{\infty} p^s(y)[k^+(y)(V(y+d) - V(y)) + k^-(y)(V(y-d) - V(y))]\,{\rm d}y \tag{18}$$

$$= \frac{\kappa d^2}{2}\langle k^+(y) + k^-(y)\rangle + \kappa d\langle y(k^+(y) - k^-(y))\rangle. \tag{19}$$

The energy thus stored in the spring is then dissipated by the probe whose heat flow is given by

$$\dot{Q}_{\rm P} \equiv \langle \dot{q}_{\rm P} \rangle = \langle (\kappa y - f_{\rm ex})\nu(y)\rangle \tag{20}$$

where

$$\nu(y) \equiv ((\kappa y - f_{\rm ex}) + k_{\rm B}T\partial_y \ln p^s(y))/\gamma. \tag{21}$$

is the local mean velocity of the probe for a given y [49, 50] which corresponds to the current arising from the motion of only the probe in (9).

3.3. Three different efficiencies

We will now focus on three different definitions of efficiency that have been proposed for motor proteins.

In the absence of an external force ($f_{\rm ex} = 0$), one can compare the energy that the motor protein transfers to the spring, $\dot{V}_n$, with its available chemical energy $\dot{\Delta}\mu$. From (15) and (17) it follows that $\dot{V}_n = \dot{Q}_{\rm P}$. The ratio of on average dissipated heat through the probe and available free energy

$$\eta_{\rm Q} \equiv \frac{\dot{Q}_{\rm P}}{\dot{\Delta}\mu} = \frac{d\kappa\langle y\nu\rangle}{v\Delta\mu} \tag{22}$$

was proposed as definition of efficiency [33]. We will see below that $\eta_{\rm Q}$ is not bounded by 1, as it has been anticipated earlier [16, 51], and therefore we will call it a pseudo efficiency. A second type of efficiency is the Stokes efficiency,

$$\eta_{\rm S} \equiv \frac{\gamma v^2}{\dot{\Delta}\mu} = \frac{d\kappa\langle y\rangle}{\Delta\mu}, \tag{23}$$

that compares the mean drag force γv the probe feels with the available chemical force. In contrast to $\eta_{\rm Q}$, $\eta_{\rm S}$ is bounded by 1 [16]. If the motor protein exerted a constant force on the probe, the Stokes efficiency would be equal to the pseudo efficiency $\eta_{\rm Q}$ because in this case the average heat dissipated by the probe is the mean drag force times d.

Finally, in the presence of an external force acting on the probe, the thermodynamic efficiency of the system is the ratio between mechanical work delivered to the external force and available free energy [10]

$$\eta_{\mathrm{T}} \equiv \frac{f_{\mathrm{ex}} v}{\dot{\Delta\mu}} = \frac{f_{\mathrm{ex}} d}{\Delta\mu}. \tag{24}$$

For $f_{\mathrm{ex}} \neq 0$, the pseudo efficiency η_{Q} can be defined as

$$\eta_{\mathrm{Q}} = \frac{\dot{Q}_{\mathrm{P}} + f_{\mathrm{ex}} v}{\dot{\Delta\mu}}. \tag{25}$$

4. Gaussian approximation

4.1. Derivation

For a comparison with the simulations and in order to gain more analytical insights, it will be convenient to have a simple approximation for the stationary distribution $p^s(y)$. For a Gaussian probability distribution

$$p^G(y) \equiv \frac{1}{\sqrt{2\pi}\sigma} \exp[-\frac{(y-\bar{y})^2}{2\sigma^2}] \tag{26}$$

the free parameters $\bar{y}$ for the mean and σ^2 for the variance can be determined by requiring that the time–derivative of these quantities as calculated with the Fokker–Planck equation (9) vanishes in the steady state. These conditions result in the following two equations for $\bar{y}$ and σ^2

$$(\kappa\bar{y} - f_{\mathrm{ex}})/\gamma = d(\bar{k}^+ - \bar{k}^-) \tag{27}$$

and

$$\begin{aligned}(\kappa\sigma^2 + \kappa\bar{y^2} - f_{\mathrm{ex}}\bar{y} - k_B T)/\gamma = d[(\bar{y} - kd\theta_+\sigma^2/k_{\mathrm{B}}T)\bar{k}^+ - (\bar{y} + kd\theta_-\sigma^2/k_{\mathrm{B}}T)\bar{k}^-] \\ + d^2(\bar{k}^+ + \bar{k}^-)/2,\end{aligned} \tag{28}$$

where we have introduced the average jump rates

$$\begin{aligned}\bar{k}^+ &\equiv \int_{-\infty}^{\infty} k^+(y) p^G(y)\,\mathrm{d}y \\ &= k^{\mathrm{eq}} \exp[\Delta\mu_{\mathrm{ATP}}/k_{\mathrm{B}}T - \kappa d^2\theta_+^2(k_{\mathrm{B}}T - \kappa\sigma^2)/2(k_{\mathrm{B}}T)^2 - \kappa d\theta_+\bar{y}/k_{\mathrm{B}}T]\end{aligned} \tag{29}$$

$$\begin{aligned}\bar{k}^- &\equiv \int_{-\infty}^{\infty} k^-(y) p^G(y)\,\mathrm{d}y \\ &= k^{\mathrm{eq}} \exp[(\Delta\mu_{\mathrm{ADP}} + \Delta\mu_{\mathrm{P_i}})/k_{\mathrm{B}}T - \kappa d^2\theta_-^2(k_{\mathrm{B}}T - \kappa\sigma^2)/2(k_{\mathrm{B}}T)^2 + \kappa d\theta_-\bar{y}/k_{\mathrm{B}}T].\end{aligned} \tag{30}$$

These equations can easily be solved numerically.

4.2. Limits $\Delta\mu \to 0$ *and* $\Delta\mu \to \infty$

Close to chemical equilibrium, i.e., $\Delta\mu = 0$, and for $f_{\mathrm{ex}} = 0$, we expand $\bar{y}$ and $\kappa\sigma^2 - k_{\mathrm{B}}T$ up to first order in $\Delta\mu$ and find

$$\bar{y} \approx A\Delta\mu + \tilde{A}(\theta_+ - \theta_-)^2\Delta\mu \tag{31}$$

and

$$\kappa\sigma^2 - k_{\rm B}T \approx B(\theta_+ - \theta_-)\Delta\mu. \tag{32}$$

The coefficients A, $\tilde{A}$ and B obtained by solving the first order of (27) and (28) are too long to be shown here.

In the limit $\Delta\mu \to \infty$ and $f_{\rm ex} = 0$, we obtain for $\bar{y}$ and $\kappa\sigma^2 - k_{\rm B}T$

$$\bar{y} \approx \frac{\Delta\mu}{\kappa d} - C\Delta\mu \exp[-\Delta\mu\theta_-/k_{\rm B}T] \tag{33}$$

and

$$\kappa\sigma^2 - k_{\rm B}T \approx D\Delta\mu \exp[-\Delta\mu\theta_-/k_{\rm B}T] \tag{34}$$

as long as $\theta_- > 0$. The coefficients

$$C = \frac{1 + \kappa d^2(\theta_+ - \theta_-)^2/4}{\gamma\kappa d^3 k^{\rm eq} \exp[(\Delta\mu_{\rm ADP} + \Delta\mu_{\rm P_i})/k_{\rm B}T]} \tag{35}$$

and

$$D = -\frac{\theta_+ - \theta_-}{2\gamma d^2 k^{\rm eq} \exp[(\Delta\mu_{\rm ADP} + \Delta\mu_{\rm P_i})/k_{\rm B}T]} \tag{36}$$

are obtained by solving (27) and (28) to first and second order in $\Delta\mu$.

4.3. Efficiencies

Within this Gaussian approximation, the average heat flow through the probe as given by (20) is calculated using the local mean velocity (21)

$$\nu(y) = (\kappa y - f_{\rm ex})/\gamma - k_{\rm B}T(y - \bar{y})/(\gamma\sigma^2). \tag{37}$$

The average over y can now be performed leading to

$$\dot{Q}_{\rm P} = (\kappa^2\sigma^2 + \kappa^2\bar{y}^2 - k_{\rm B}T\kappa - 2\kappa f_{\rm ex}\bar{y} + f_{\rm ex}^2)/\gamma. \tag{38}$$

This expression is used to determine $\eta_{\rm Q}$ in this approximation as

$$\eta_{\rm Q} = d\kappa \frac{\kappa\sigma^2 - k_{\rm B}T + \kappa\bar{y}^2 - f_{\rm ex}\bar{y}}{\Delta\mu(\kappa\bar{y} - f_{\rm ex})} \tag{39}$$

with $\bar{y}$ and σ^2 being the solution of (27) and (28) for given $\Delta\mu$ and $k^{\rm eq}$.

For small $\Delta\mu$, using (31) and (32), $\eta_{\rm Q}$ takes the form

$$\eta_{\rm Q} \approx \frac{dB(\theta_+ - \theta_-)}{(A + \tilde{A}(\theta_+ - \theta_-)^2)\Delta\mu} + \kappa dA + \kappa d\tilde{A}(\theta_+ - \theta_-)^2. \tag{40}$$

If $\theta_+ \neq \theta_-$, $\eta_{\rm Q}$ diverges for vanishing $\Delta\mu$. For $\theta_+ > \theta_-$, $\eta_{\rm Q}$ can become negative due to those jumps of the motor protein that occur when the previous diffusion of the probe has resulted in $y < -0.5d$. Then, the energy stored in the spring is dissipated by the motor protein during jumping.

In the limit of large $\Delta\mu$, we use (34) and (35) to obtain

$$\eta_{\rm Q} \approx 1 - \kappa dC \exp[-\Delta\mu\theta_-/k_{\rm B}T] + \frac{dD \exp[-\Delta\mu\theta_-/k_{\rm B}T]}{\Delta\mu/(\kappa d) - C\Delta\mu \exp[-\Delta\mu\theta_-/k_{\rm B}T]} \tag{41}$$

Table 1. Values of the model parameters used for the simulation and the Gaussian approximation.

γ (k_BTs/d^2)	κ (k_BT/d^2)	k^{eq}/c^{eq}_{ATP} ($M^{-1}s^{-1}$)
0.407	40	$3 \cdot 10^7$

which approaches 1.

The Stokes efficiency in the Gaussian approximation without an external force is simply given by

$$\eta_S = \frac{d\kappa\bar{y}}{\Delta\mu}. \tag{42}$$

For $\kappa\sigma^2 > k_BT$, which is the case for $\theta_+ < 0.5$, the Stokes efficiency is always smaller than η_Q. For vanishing $\Delta\mu$, η_S approaches a finite value, $\eta_S \approx d\kappa A + d\kappa\tilde{A}(\theta_+ - \theta_-)^2$, while for $\Delta\mu \to \infty$ it also converges to 1.

5. Results

In this section, we study the three efficiencies for our hybrid model as functions of the chemical energy $\Delta\mu$, the absolute concentrations of the nucleodides, i.e. k^{eq}, the external force f_{ex} and the load sharing factor θ_+. The data are obtained from simulations, using a Gillespie algorithm [52] similar to [37] with the motion of the probe being spatially discretized in steps of $\Delta x = d/1000$, and compared with the Gaussian approximation.

We use model parameters as given in table 1 which are motivated by experimental results for the F_1–ATPase as described in section 6 below. The load sharing factor θ_+ remains as a free parameter.

Simulated trajectories with the same nucleotide concentrations as used in the experiment [33] are shown in figure 2. In the presence of low nucleotide concentrations only few backward jumps of the motor protein take place and the trajectory of the probe shows an almost staircase like form. For high nucleotide concentrations, following a forward step the motor often performs a backward jump. Such a sequence of two jumps is not necessarily visible in the trajectory of the probe which remains almost linear.

5.1. Pseudo efficiency η_Q

We will first investigate the pseudo efficiency η_Q as a function of $\Delta\mu$, k^{eq} and θ_+. We extract $\dot{Q}_P$ from the numerical data by averaging over one sufficiently long trajectory. The results are shown in figure 3. The most striking fact of these data is the observation that η_Q is larger than 1 for small enough $\Delta\mu$ and θ_+ which shows up in the Gaussian approximation as well. This effect can be understood as follows. In a jump, the motor protein can take heat from the solution in order to change the internal energy of the spring by an amount larger than $\Delta\mu$. If, subsequently, the probe dissipates this internal

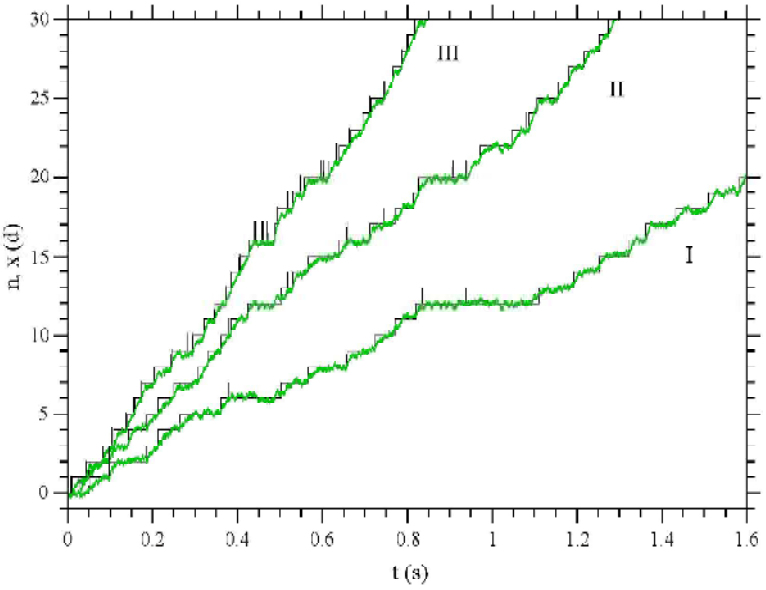

Figure 2. Trajectories of the molecular motor (black) and the attached probe particle (green) obtained from the simualtion (without external force). In the presence of low nucleotide concentrations (I) the trajectory of the probe exhibits a more stepwise form while it becomes almost linear for high nucleotide concentrations (III). The parameters are $\theta_+ = 0.1$, (I): $c_{\mathrm{ATP}} = 0.4\,\mu$M, $c_{\mathrm{ADP}} = 0.4\,\mu$M, $c_{\mathrm{P_i}} = 1$ mM, (II): $c_{\mathrm{ATP}} = 2\,\mu$M, $c_{\mathrm{ADP}} = 2\,\mu$M, $c_{\mathrm{P_i}} = 1$ mM, (III): $c_{\mathrm{ATP}} = 100\,\mu$M, $c_{\mathrm{ADP}} = 100\,\mu$M, $c_{\mathrm{P_i}} = 1$ mM. For all parameter sets we have $\Delta\mu = 19.14\,k_{\mathrm{B}}T$. The nucleotide concentrations are the same as used in the experiment [33] shown in figure 8 with the same labelling (I-III) below.

energy of the spring as heat back into the environment, $\dot{Q}_{\mathrm{P}}$ can indeed become larger than $\dot{\Delta\mu}$ without any violation of the second law. Using the obtained parameter for the spring constant κ, the motor protein transfers $20\,k_{\mathrm{B}}T$ to the spring if it starts the jump from the minimum of the harmonic potential. For small values of θ_+, the forward jump rate of the motor protein depends only weakly on the current position of the probe as shown in figure 4. Therefore, jumps will occur even if the associated change of internal energy of the spring, ΔV, is larger than $\Delta\mu$. For rather small k^{eq}, backward jumps are rare and the probe relaxes to the potential minimum between successive forward jumps (see data set I in figure 2). This leads to $\dot{V}_n > \dot{\Delta\mu}$ on average and hence to $\eta_Q > 1$ for $\Delta\mu$ considerably smaller than $20\,k_{\mathrm{B}}T$ as shown in figure 3. As the value of θ_+ increases, η_{Q} decreases because the forward jumps of the motor protein are suppressed. On average, in this case the motor protein jumps only if the probe has diffused forward and exerts a pulling force on the motor through the spring.

Increasing the absolute concentrations of the nucleotides, i.e., increasing k^{eq}, results in more forward but also more backward jumps, which can be seen for data set III in figure 2. For small $\Delta\mu$, the occasional backward jumps follow especially those forward jumps for which the change of internal energy of the spring has been larger than $\Delta\mu$, leading to a smaller η_{Q}.

In the limit of large $\Delta\mu$, the motor protein jumps even when the spring is previously

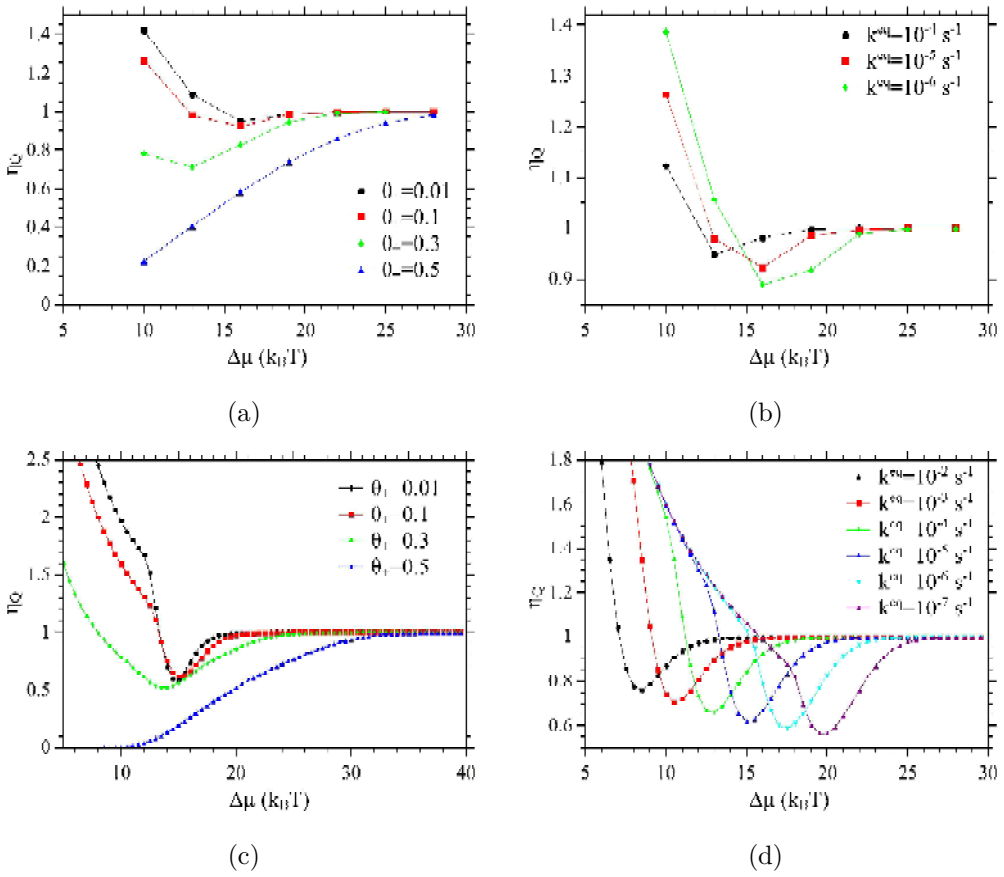

Figure 3. Pseudo efficiency $\eta_{\rm Q}$ from the simulation, (a) and (b); and within the Gaussian approximation, (c) and (d). (a) and (c): $\eta_{\rm Q}$ as a function of $\Delta\mu$ for different values of the load sharing factor θ_+ and fixed $k^{\rm eq} = 10^{-5}{\rm s}^{-1}$. (b) and (d): $\eta_{\rm Q}$ as a function of $\Delta\mu$ for different values of $k^{\rm eq}$ with fixed $\theta_+ = 0.1$. The remaining parameters are $\kappa = 40 k_{\rm B}T/d^2$, $\gamma = 0.407 k_{\rm B}T{\rm s}/d^2$. In the simulation, the error is of the order of the symbol size.

stretched which can result in changes of the internal energy of the spring by an amount larger than $20\,k_{\rm B}T$. The coupling between the motor protein and the probe induces a balancing effect between the forward motion of the motor protein and the drag of the probe maintaining a typical $\dot{V}$ that turns out to be approximately $\dot{\Delta\mu}$, leading to $\eta_{\rm Q} \simeq 1$.

5.2. Stokes efficiency $\eta_{\rm S}$

We also obtain the Stokes efficiency (23) from the simulated trajectories and the Gaussian approximation as shown in figure 5. Characteristically, starting close to 0 for small $\Delta\mu$, $\eta_{\rm S}$ monotonically increases with $\Delta\mu$ reaching 1 for $\Delta\mu \to \infty$. For small $\Delta\mu$, the trajectory of the probe shows a staircase form with small average velocity leading to small values of the Stokes efficiency in contrast to values of the pseudo efficiency $\eta_{\rm Q} > 1$. For large $\Delta\mu$, the probe does not relax to the potential minimum between consecutive jumps resulting in a more linear trajectory of the probe as if it was exposed

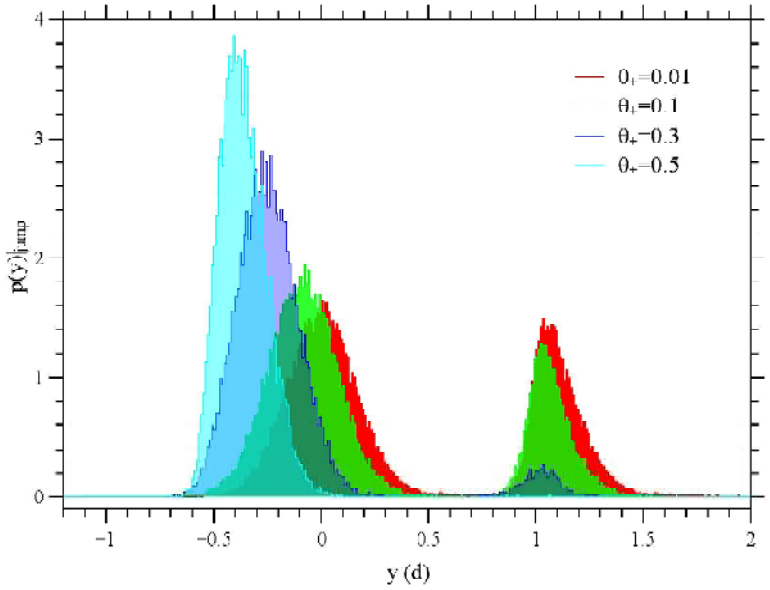

Figure 4. Probability distribution $p(y)_{|\text{jump}}$ of the distance y just before a jump of the motor protein for several values of θ_+ at $\Delta\mu = 13k_BT$ and $k^{\text{eq}} = 10^{-5}\text{s}^{-1}$. For small θ_+, the forward jumps of the motor protein are almost independent of the position of the probe resulting in a peak at $y \simeq 0$ whereas for larger θ_+ the peak clearly shifts to $y < 0$ implying that the motor protein prefers to jump when the probe has diffused ahead. The peaks around $y = 1$ indicate backward jumps which take place more often in the case of small θ_+ when the backward rate is more sensitive to the position of the probe.

to an almost constant force. In this limit of an almost linear motion of the probe, the pseudo efficiency becomes the Stokes efficiency. As η_S is bounded by 1, η_Q can not reach values larger than 1 in this limit either.

Increasing the load sharing factor θ_+ results in decreasing average velocities. Therefore, the Stokes efficiency also decreases which can be seen in figures 5 (a) and (c). With increasing absolute concentrations of nucleotides, i.e., with increasing k^{eq}, the average velocity and therefore also the Stokes efficiency at fixed $\Delta\mu$ increases as shown in figures 5 (b) and (d).

5.3. Thermodynamic efficiency η_T

The thermodynamic efficiency of the system can be studied only if an external force is applied to the probe. As an illustrative example, for fixed $\Delta\mu = 19k_BT$, we examine the thermodynamic efficiency in the presence of external forces smaller than the stall force as shown in figure 6. The thermodynamic efficiency increases linearly with f_{ex} and reaches 1 at the stall force which is possible only due to the tight mechanochemical coupling in this model. In figure 6 we also show the pseudo efficiency η_Q as defined in (25) in the presence of external forces. While η_Q is almost independent of the external force, the contribution from the dissipated heat, $\dot{Q}_P/\dot{\Delta\mu}$, decreases linearly with f_{ex} and

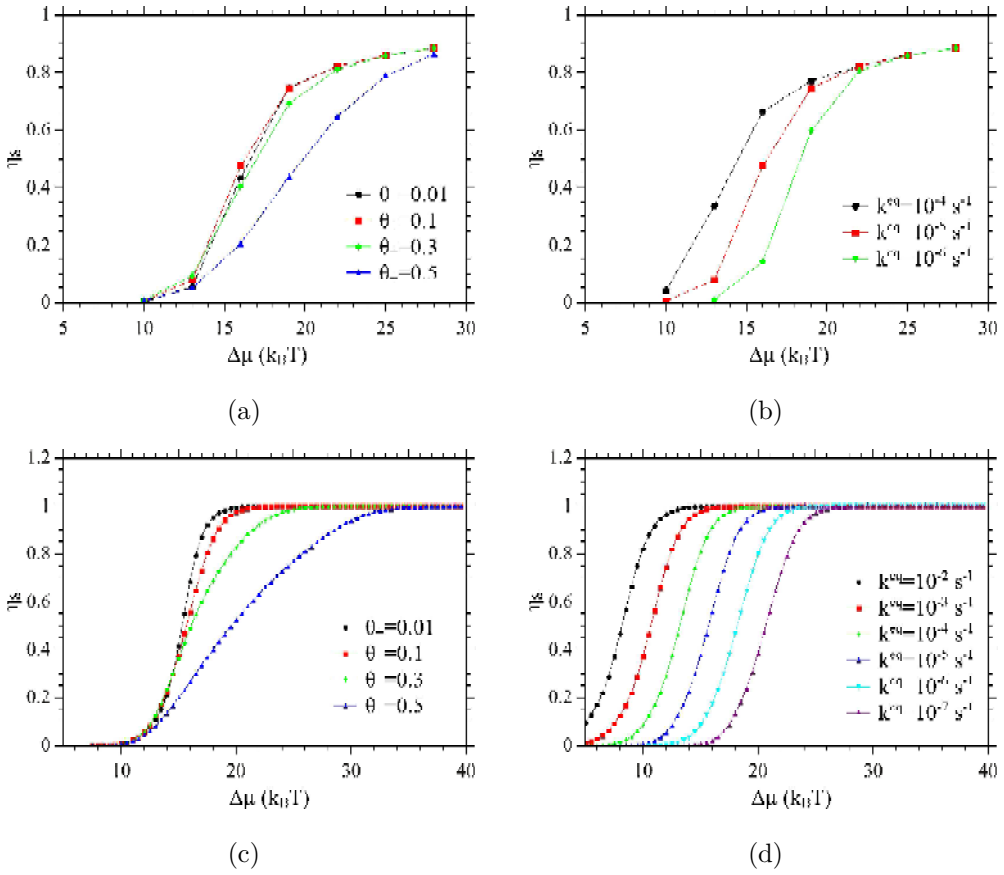

Figure 5. (a) Stokes efficiency η_S from the simulation, (a) and (b); and within the Gaussian approximation, (c) and (d). The data is obtained from the same trajectories used to obtain η_Q in figure 3 (a) and (b). (a) and (c): η_S as a function of $\Delta\mu$ for different values of the load sharing factor θ_+ and fixed $k^{eq} = 10^{-5}s^{-1}$. (b) and (d): η_S as a function of $\Delta\mu$ for different values of k^{eq} for fixed $\theta_+ = 0.1$.

reaches zero at the stall force.

At stall conditions, the work corresponding to the stall force refers to the maximum work the motor protein can convert on average. In the simulation, we find that applying $f_{ex} = \Delta\mu/d$ generates a diffusive motion of the motor protein with $v \simeq 0$ and $\dot{Q}_P \simeq 0$ for various values of θ_+ and $\Delta\mu$, including the ones with $\eta_Q > 1$ and $\eta_Q < 1$. This observation implies that the motor protein seems in principle to be able to convert the full $\Delta\mu$ into extractable work. In our model, where the motor interacts with the external force only via the spring, this result is not trivial, as it would have been if we had applied f_{ex} directly to the motor. Under these conditions, $p^s(y)$ is Gaussian with $\langle y\rangle = \Delta\mu/(dk)$ and the same variance as the Boltzmann-distribution in equilibrium, $\sigma^2 = k_BT/\kappa$.

Within the Gaussian approximation we can insert $f_{ex} = \Delta\mu/d$ in (27) and (28). With $\kappa\sigma^2 = k_BT$, $\bar{y} = \Delta\mu/(d\kappa)$, i.e., $v = 0$ is a solution for $f_{ex} = \Delta\mu/d$, implying that also in the Gaussian approximation the motor protein is able to convert the full $\Delta\mu$ into extractable work for any values of the load sharing factors given that $\theta_+ + \theta_- = 1$.

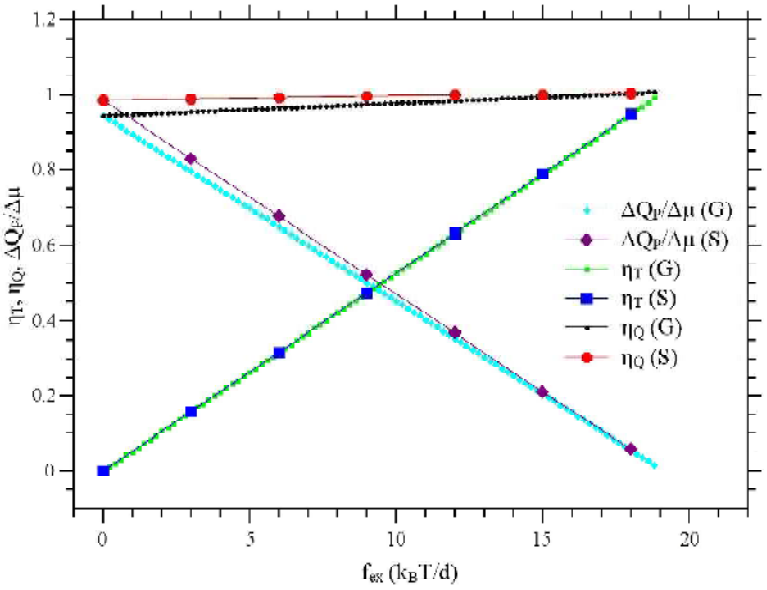

Figure 6. Pseudo efficiency η_Q (red and black dots), thermodynamic efficiency η_T (green and blue squares) and dissipated heat ΔQ_P per $\Delta\mu$ (cyan and purple diamonds) as functions of f_{ex} for fixed $\Delta\mu = 19k_BT$, $\theta_+ = 0.1$ and $k^{eq} = 10^{-5}s^{-1}$. The plot contains data from the simulation (S) as well as from the Gaussian approximation (G).

6. Case study: F_1–ATPase

In this section, we apply our hybrid model to the F_1–ATPase and compare the simulations with recent experimental data [33, 34, 35].

6.1. Model parameters

For a quantitative comparison we have to map the rotary motion of the F_1–ATPase to our linear model and determine the model parameters. In our model, one jump of the motor protein covering a distance d corresponds to a rotation of the γ shaft of 120°. Using large probe particles like polystyrene beads or actin filaments, the substeps in one 120° rotation are not resolved experimentally. Therefore, we will omit the substeps here, too. We assume that the temperature of the solution is $T \simeq 24°C$ and that the probe consists of two beads of diameter 287nm [33]. The friction coefficient of the probe can be calculated using the formula for the rotational frictional coefficient Γ from [36, 37] with the viscosity of water ($\eta \simeq 0.001 Ns/m^2$). The frictional torque $N = \Gamma\dot{\varphi}$ acting on the probe with angular velocity $\dot{\varphi}$ corresponds to a frictional force

$$f_{fr} = \frac{\Gamma}{r^2}\dot{x} = \gamma\dot{x} \tag{43}$$

acting on the probe at distance r from the γ shaft. Within one 120° rotation, the probe at distance r covers $d = 2\pi r/3$. For the linear model, the friction coefficient γ can be

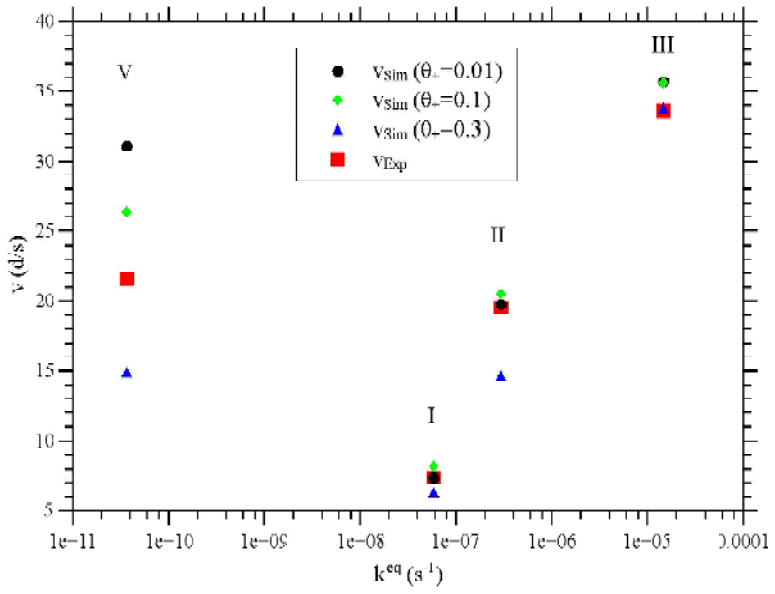

Figure 7. Comparison of the mean velocities observed experimentally [33] (red squares) and in the simulation for several load sharing factors θ_+ (black dots, green diamonds and blue triangles). The labelling I, II, III, V refers to the corresponding parameter sets in figure 8.

calculated as

$$\gamma = \frac{\Gamma}{r^2} = \frac{4\pi^2\Gamma}{9d^2} \tag{44}$$

leading to $\gamma = 0.407\, k_B T\, s/d^2$.

Following the mass action law assumption, the equilibrium transition rate k^{eq} is supposed to depend linearly on the concentrations of nucleotides in the solvent. For low ATP concentrations ($c_{ATP} \simeq 10^{-6}$M), the mean velocity of the motor protein is dominated by the rate of ATP binding. In the one–step model this feature holds for all concentrations. Therefore we choose k^{eq} to be the experimentally determined rate of ATP binding $k^{eq} \simeq 3 \cdot 10^7 M^{-1} s^{-1} c^{eq}_{ATP}$[42]. For known nonequilibrium concentrations of nucleotides like in the experiments, the structure of the transition rates (5) and (6) leaves the choice of the equilibrium concentrations arbitrary as long as they obey

$$\frac{c^{eq}_{ATP}}{c^{eq}_{ADP} c^{eq}_{P_i}} \simeq 4.89 \cdot 10^{-6} \frac{1}{M} \tag{45}$$

for $T = 23°C$ and pH 7 [37]. For given k^{eq} and $\Delta\mu$, one possible choice of the nonequilibrium concentrations of nucleotides is $c_{ADP} = c^{eq}_{ADP}$, $c_{P_i} = c^{eq}_{P_i}$ and $c_{ATP} = c^{eq}_{ATP} \exp[\Delta\mu/k_B T]$ which was used for the simulation and the Gaussian approximation.

In order to determine the spring constant κ and the load sharing factor θ_+ we use both the experimental data of the mean velocities [33] and the histogram of the angular position of the probe at a jump [35]. While both data sets depend on both parameters, the velocity, especially for large k^{eq}, is more sensitive to κ whereas the peak position of the histogram mainly depends on θ_+. Therefore, we primarily use the velocity data to

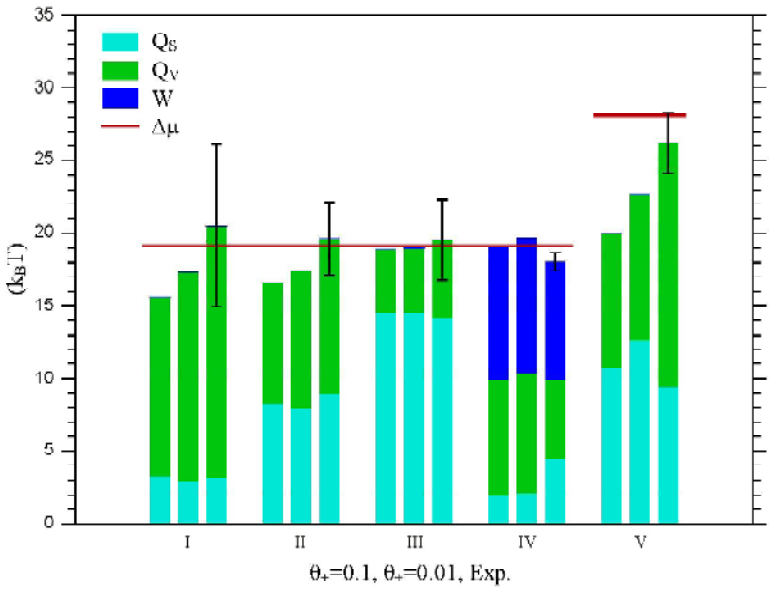

Figure 8. Average heat Q_P released through the probe (green and cyan) and work $W \equiv f_\mathrm{ex} d$ against the external force (blue) compared to the available free energy per step $\Delta\mu$ (red line). The dissipated heat of the probe is split into two contributions Q_S and Q_V according to the two terms of the Harada–Sasa relation (A.3). The contribution from the linear motion with constant mean velocity, Q_S (cyan), appears in the numerator of the Stokes efficiency while Q_V (green) is the contribution due to the non–uniform jumping motion of the motor protein. In each of the five parameter sets labelled by I-V, the left and the central bar represent results from the simulation for $\theta_+ = 0.1$ and $\theta_+ = 0.01$, respectively, while the right bar shows the experimental results and error bars from [33]. The following parameters were used in the five cases: (I) $c_\mathrm{ATP} = 0.4\,\mu$M, $c_\mathrm{ADP} = 0.4\,\mu$M, $c_{\mathrm{P_i}} = 1$ mM, i.e, $k^\mathrm{eq} = 5.87 \cdot 10^{-8}\,\mathrm{s}^{-1}$ and $\Delta\mu = 19.14\,k_\mathrm{B}T$; (II) $c_\mathrm{ATP} = 2\,\mu$M, $c_\mathrm{ADP} = 2\,\mu$M, $c_{\mathrm{P_i}} = 1$ mM, i.e, $k^\mathrm{eq} = 2.93{\cdot}10^{-7}\,\mathrm{s}^{-1}$ and $\Delta\mu = 19.14\,k_\mathrm{B}T$; (III) $c_\mathrm{ATP} = 100\,\mu$M, $c_\mathrm{ADP} = 100\,\mu$M, $c_{\mathrm{P_i}} = 1$ mM, i.e, $k^\mathrm{eq} = 1.47 \cdot 10^{-5}\,\mathrm{s}^{-1}$ and $\Delta\mu = 19.14\,k_\mathrm{B}T$; (IV) $c_\mathrm{ATP} = 2\,\mu$M, $c_\mathrm{ADP} = 2\,\mu$M, $c_{\mathrm{P_i}} = 1$ mM, $f_\mathrm{ex} = 9.27\,k_BT/d$, i.e, $k^\mathrm{eq} = 2.93 \cdot 10^{-7}\,\mathrm{s}^{-1}$ and $\Delta\mu = 19.14\,k_\mathrm{B}T$; (V) $c_\mathrm{ATP} = 2\,\mu$M, $c_\mathrm{ADP} = 0.5\,\mu$M, $c_{\mathrm{P_i}} = 0.5\,\mu$M, i.e, $k^\mathrm{eq} = 3.67 \cdot 10^{-11}\,\mathrm{s}^{-1}$ and $\Delta\mu = 28.12\,k_\mathrm{B}T$;

fit κ and determine the load sharing factor θ_+ by comparing the peak position of the experimental histogram [35] with the left peak position of the corresponding histograms obtained by our simulation as the ones shown in figure 4.

As a result, we obtain $\kappa = 40 \pm 5\,k_\mathrm{B}T/d^2$ and a value of θ_+ in the range $0.1 \lesssim \theta_+ \lesssim 0.3$. In figure 7, we show how for this value of κ changing the load sharing factor affects the mean velocity for which we get the best overall agreement for $\theta_+ = 0.1$. For later purposes, we also include data for $\theta_+ = 0.01$.

6.2. Comparison of efficiencies with experimental data

Experimentally, the heat flow of the probe is determined using the Harada–Sasa relation [53]. In the appendix, we show that this heat flow is equal to $\dot{Q}_\mathrm{P}$ as defined in (20).

In figure 8, we plot the average heat released through the probe per step, Q_P, plus the work against the external force, W, obtained by the simulation for $\kappa = 40\,k_BT/d^2$ and $\theta_+ = 0.1$ and compare it with the experimental results [33]. We find quite good agreement between theory and experiment for the parameter sets I-IV where either the maximum deviation is 15% (II-IV) or our theoretical value is included in the experimental error range (I). As an aside, we note that for the parameter sets I-III (without external force) also the simulated mean velocities coincide well with the experimental values with a maximum deviation of 10% as shown in figure 7. For illustrative purposes, we also plot Q_P plus W for $\theta_+ = 0.01$ which shows better agreement with the experimental data (but is not consistent with the range of θ_+ obtained in section 6.1).

Discrepancies between our theory and the experiment are visible in figures 7 and 8 where for parameter set V both the average velocity and the pseudo efficiency deviate significantly from the experimental values for $\kappa = 40\,k_BT/d^2$ and $\theta_+ = 0.1$. For $\Delta\mu = 28.12 k_BT$ corresponding to the data set V in figure 8, the probe just reaches the potential minimum between consecutive jumps of the motor protein. Therefore on average at most $20 k_BT$ can be transferred to the spring leading to $\eta_Q \simeq 0.7$, which is less than the experimental value. This discrepancy is most likely due to the fact that we have omitted substeps in our model. In the simulation, the average velocity then does not show saturation as one would expect it to result from the hydrolysis step [42] which should be experimentally observable at the higher concentrations used in [33].

The confinement of θ_+ to the range $0.1 \lesssim \theta_+ \lesssim 0.3$ implies on the one hand that the potential of mean force of the motor protein should be asymmetric and on the other hand that asymmetric potentials with a barrier state close to the initial state seem to enhance the ability of the motor protein to perform work on the spring, in accordance with [54]. If θ_+ was larger, η_Q would decrease and the experimentally determined values of η_Q would not be reached in the simulation. If θ_+ was smaller, η_Q would approach the experimental values better, however, the distribution of the position of the probe just before a jump as shown in figure 4 would then no longer coincide with the experimentally observed distribution (see [35]).

Information about the thermodynamic efficiency of the motor protein can be gained by applying an external force at the probe. In our simulation, the stall force is found to be $f_{ex} = \Delta\mu/d$, implying that the motor protein is able to convert the full $\Delta\mu$ into extractable work without dissipation in accordance with the experiments performed in [34].

7. Conclusion

In summary, we have discussed a simple generic model which includes the elastic linker between the probe particle and the molecular motor. Properties of the motor become typically accessible only through the observation of the motion of the probe. We have then focussed on discussing three types of efficencies within this model using both

simulations and a Gaussian approximation to the stationary distribution for the distance between motor and probe. The genuine thermodynamic efficiency is non-zero only if an external force is applied to the probe. The Stokes efficiency deviates from 1 due to the discrete nature of the motor steps which become less relevant with increasing ATP concentration. A pseudo efficiency measuring how much of the free energy of ATP hydrolysis ends up in loading the elastic element can even become larger than 1 close to equilibrium and for a barrier state close to the initial state.

Applying this minimal model to recent experimental data for the F_1–ATPase we find overall good agreement except for those parameters where especially the P_i concentration is very small. In general, one should consider ATP binding and ATP hydrolysis as two separate steps. Such a refinement as well as a splitting of the 120° rotation into two steps of 90° and 30° as experimentally observed using much smaller probe particles does not pose new conceptual challenges to the present framework and will be pursued elsewhere.

Appendix A. Equivalence of heat flow $\dot{Q}_P$ with the one inferred from the Harada–Sasa relation

Experimentally, the heat flow caused by the probe has been inferred from measuring the autocorrelation function $C_{\dot{x}}(\tau) = \langle \dot{x}(t+\tau)\dot{x}(t)\rangle - v^2$ and the linear response function

$$R_{\dot{x}}(\tau) \equiv \frac{\delta\langle \dot{x}(t+\tau)\rangle}{\delta h(t)}|_{h=0} \tag{A.1}$$

of the velocity of the probe to a small external perturbation $h(t)$ of the probe within the steady state [33]. The heat flow is then given by an equality derived by Harada and Sasa [53]

$$\begin{aligned}\dot{Q}^{\mathrm{HS}} &= \gamma v^2 + \gamma \int_{-\infty}^{\infty} \frac{\mathrm{d}\omega}{2\pi}[\tilde{C}_{\dot{x}}(\omega) - 2k_{\mathrm{B}}T\,\mathrm{Re}\,(\tilde{R}_{\dot{x}}(\omega))] \\ &= \gamma v^2 + \gamma[C_{\dot{x}}(0) - 2k_{\mathrm{B}}T R_{\dot{x}}(0)] \qquad (A.2)\\ &\equiv \dot{Q}_{\mathrm{S}} + \dot{Q}_{\mathrm{V}}, \qquad (A.3)\end{aligned}$$

with $\tilde{C}_{\dot{x}}$ and $\tilde{R}_{\dot{x}}$ being the Fourier transforms of $C_{\dot{x}}$ and $R_{\dot{x}}$. Using a path weight approach described in [55] applied to our system, the response function follows as

$$R_{\dot{x}}(\tau) = \frac{1}{2k_{\mathrm{B}}T}\langle \dot{x}(t+\tau)[\dot{x}(t) - (\kappa y(t) - f_{\mathrm{ex}})/\gamma]\rangle. \tag{A.4}$$

Inserting $C_{\dot{x}}$ and this $R_{\dot{x}}$ into (A.2), one immediately finds

$$\dot{Q}^{\mathrm{HS}} = \langle \dot{x}(\kappa y - f_{\mathrm{ex}})\rangle \tag{A.5}$$

which is equal to $\dot{Q}_{\mathrm{P}}$ in (20).

References

[1] J. Howard. *Mechanics of Motor Proteins and the Cytoskeleton.* Sinauer, New York, 1 edition, 2001.

[2] M. Schliwa. *Molecular Motors.* Wiley-VCH, Weinheim, 2003.

[3] F. Jülicher, A. Ajdari, and J. Prost. Modeling molecular motors. *Rev. Mod. Phys.*, 69(4):1269–1282, 1997.

[4] P. Reimann. Brownian motors: noisy transport far from equilibrium. *Phys. Rep.*, 361:57, 2002.

[5] A. B. Kolomeisky and M. E. Fisher. Molecular Motors: A Theorist's Perspective. *Ann. Rev. Phys. Chem.*, 58:675–695, 2007.

[6] A. W. C. Lau, D. Lacoste, and K. Mallick. Non-equilibrium fluctuations and mechanochemical couplings of a molecular motor. *Phys. Rev. Lett.*, 99:158102, 2007.

[7] S. Liepelt and R. Lipowsky. Kinesin's network of chemomechanical motor cycles. *Phys. Rev. Lett.*, 98:258102, 2007.

[8] R. Lipowsky, S. Liepelt, and A. Valleriani. Energy conversion by molecular motors coupled to nucleotide hydrolysis. *J. Stat. Phys.*, 135:951–975, 2009.

[9] R. D. Astumian. Thermodynamics and kinetics of molecular motors. *Biophys. J.*, 98:2401–2409, 2010.

[10] A. Parmeggiani, F. Jülicher, A. Ajdari, and J. Prost. Energy transduction of isothermal ratchets: Generic aspects and specific examples close to and far from equilibrium. *Phys. Rev. E*, 60:2127, 1999.

[11] J. M. R. Parrondo and B. J. De Cisneros. Energetics of Brownian motors: a review. *Applied Physics A*, 75:179, 2002.

[12] U. Seifert. Efficiency of autonomous soft nano-machines at maximum power. *Phys. Rev. Lett.*, 106:020601, 2011.

[13] A. Efremov and Z. Wang. Universal optimal working cycles of molecular motors. *Phys. Chem. Chem. Phys.*, 13:6223–6233, 2011.

[14] K. Kawaguchi and M. Sano. Efficiency of free energy transduction in autonomous systems. *J. Phys. Soc. Japan*, 80:083003, 2011.

[15] I. Derenyi, M. Bier, and R. D. Astumian. Generalized efficiency and its application to microscopic engines. *Phys. Rev. Lett.*, 83:903, 1999.

[16] H. Wang and G. F. Oster. The Stokes efficiency for molecular motors and its applications. *Europhys. Lett.*, 57:134, 2002.

[17] D. Suzuki and T. Munakata. Rectification efficiency of a Brownian motor. *Phys. Rev. E*, 68, 2003.

[18] H. Wang. Chemical and mechanical efficiencies of molecular motors and implications for motor mechanisms. *J. Phys. Cond. Mat.*, 17:S3997–S4014, 2005.

[19] M. Qian, X. Zhang, R. J. Wilson, and J. Feng. Efficiency of Brownian motors in terms of entropy production rate. *EPL*, 84, 2008.

[20] E. Boksenbojm and B. Wynants. The entropy and efficiency of a molecular motor model. *J. Phys. A: Math. Theor.*, 42, 2009.

[21] H. Noji, R. Yasuda, M. Yoshida, and K. Kinosita. Direct observation of the rotation of F1-ATPase. *Nature*, 386:299–302, 1997.

[22] R. S. Rock, S. E. Rice, A. L. Wells, T. J. Purcell andJ. A. Spudich, and H. L Sweeney. Myosin VI is a processive motor with a large step size. *Proc. Natl. Acad. Sci. U.S.A.*, 98:13655, 2001.

[23] H. Itoh, Takahashi A., K. Adachi, H. Noji, R. Yasuda, M. Yoshida, and K. Kinosita. Mechanically driven ATP synthesis by F1-ATPase. *Nature*, 427:465–468, 2004.

[24] N. J. Carter and R. A. Cross. Mechanics of the kinesin step. *Nature*, 435:308, 2005.

[25] C. S. Peskin and T. C. Elston. The role of protein flexibility in molecular motor function: Coupled diffusion in a tilted periodic potential. *SIAM J. Appl. Math.*, 60:842–867, 2000.

[26] C. S. Peskin, D. You, and T. C. Elston. Protein flexibility and the correlation ratchet. *SIAM J. Appl. Math.*, 61:776–791, 2000.

[27] Y. Chen. Theoretical formalism for kinesin motility i. bead movement powered by single one-headed kinesins. *Biophys. J*, 78:313–321, 2000.

[28] Y. Chen, B. Yan, and R. J. Rubin. Fluctuations and randomness of movement of the bead powered by a single kinesin molecule in a force-clamped motility assay: Monte carlo simulations. *Biophys. J.*, 83:2360–2369, 2002.

[29] K. B. Zeldovich, J. F. Joanny, and J. Prost. Motor proteins transporting cargos. *Eur. Phys. J. E*, 17:155–163, 2005.

[30] H. Wang and H. Zhou. Stokes efficiency of molecular motor-cargo systems. *Abstract and Applied Analysis*, 2008, 2008.

[31] A. Kunwar, M. Vershinin, J. Xu, and S. P. Gross. Stepping, strain gating, and an unexpected force-velocity curve for multiple-motor-based transport. *Curr. Biol.*, 18:1173–1183, 2008.

[32] S. Bouzat and F. Falo. The influence of direct motor-motor interaction in models for cargo transport by a single team of motors. *Phys. Biol.*, 7, 2010.

[33] S. Toyabe, T. Okamoto, T. Watanabe-Nakayama, H. Taketani, S. Kudo, and E. Muneyuki. Nonequilibrium energetics of a single F1-ATPase molecule. *Phys. Rev. Lett.*, 104:198103, 2010.

[34] S. Toyabe, T. Watanabe-Nakayama, T. Okamoto, S. Kudo, and E. Muneyuki. Thermodynamic efficiency and mechanochemical coupling of F1-ATPase. *Proc. Natl. Acad. Sci. U.S.A.*, 108:17951–17956, 2011.

[35] S. Toyabe, H. Ueno, and E. Muneyuki. Recovery of state-specific potential of molecular motor from single-molecule trajectory. *EPL*, 97:40004, 2012.

[36] K. Hayashi, H. Ueno, R. Iino, and H. Noji. Fluctuation theorem applied to F1-ATPase. *Phys. Rev. Lett.*, 104:218103, 2010.

[37] P. Gaspard and E. Gerritsma. The stochastic chemomechanics of the F1-ATPase molecular motor. *J. Theor. Biol.*, 247:672–686, 2007.

[38] E. Gerritsma and P. Gaspard. Chemomechanical coupling and stochastic thermodynamics of the F1-ATPase molecuar motor with an applied external torque. *Biophys. Rev. Lett.*, 5:163–208, 2010.

[39] H. Wang and G. Oster. Energy transduction in the F1 motor of ATP synthase. *Nature*, 396:279–282, 1998.

[40] S. X. Sun, H. Wang, and G. Oster. Asymmetry in the F1-ATPase and its implications for the rotational cycle. *Biophys. J.*, 86:1373–1384, 2004.

[41] D. Okuno, R. Iino, and H. Noji. Rotation and structure of FoF1-ATP synthase. *J Biochem*, 149:655–664, 2011.

[42] R. Yasuda, H. Noji, M. Yoshida, K. Kinosita Jr., and H. Itoh. Resolution of distinct rotational substeps by submillisedcond kinetic analysis of F1-ATPase. *Nature*, 410:898, 2001.

[43] R. Yasuda, H. Noji, K. Kinosita, and M. Yoshida. F1-ATPase is a highly efficient molecular motor that rotates with discrete 120 degree steps. *Cell*, 93:1117, 1998.

[44] E. Muneyuki, T. Watanabe-Nakayama, T. Suzuki, M. Yoshida, T. Nishizaka, and H. Noji. Single molecule energetics of F1-ATPase motor. *Biophys. J.*, 92:1806–1812, 2007.

[45] M. E. Fisher and A. B. Kolomeisky. The force exerted by a molecular motor. *Proc. Natl. Acad. Sci. U.S.A.*, 96:6597, 1999.

[46] K. Sekimoto. Langevin equation and thermodynamics. *Prog. Theor. Phys. Supp.*, 130:17, 1998.

[47] U. Seifert. Stochastic thermodynamics: Principles and perspectives. *Eur. Phys. J. B*, 64:423–431, 2008.

[48] U. Seifert. Stochastic thermodynamics of single enzymes and molecular motors. *Eur. Phys. J. E*, 34:26, 2011.

[49] T. Hatano and S. Sasa. Steady-state thermodynamics of Langevin systems. *Phys. Rev. Lett.*, 86:3463, 2001.

[50] T. Speck and U. Seifert. Restoring a fluctuation-dissipation theorem in a nonequilibrium steady state. *Europhys. Lett.*, 74:391, 2006.

[51] K. Kinosita, K. Adachi, and H. Itoh. Rotation of F1-ATPase: How an ATP- driven molecular machine may work. *Annu. Rev. Biophys. Biomol. Struct.*, 33:245–268, 2004.

[52] D. T. Gillespie. *Markov Processes*. Academic Press, San Diego, 1992.

[53] T. Harada and S. Sasa. Equality connecting energy dissipation with a violation of the fluctuation-response relation. *Phys. Rev. Lett.*, 95:130602, 2005.

[54] T. Schmiedl and U. Seifert. Efficiency of molecular motors at maximum power. *EPL*, 83:30005,

2008.

[55] U. Seifert and T. Speck. Fluctuation-dissipation theorem in nonequilibrium steady states. *EPL*, 89:10007, 2010.